Supplementary Materials for

Sub-daily natural CO_2 flux simulation based on satellite data: diurnal and seasonal pattern comparisons to anthropogenic CO_2 emissions in the Greater Tokyo Area

Qiao Wang [1,*], Ryoichi Imasu [1], Yutaka Arai [1], Satoshi Ito [1], Yasuko Mizoguchi [2], Hiroaki Kondo [3,4] and

Jingfeng Xiao [5]

1 Atmosphere and Ocean Research Institute, The University of Tokyo, 5-1-5 Kashiwanoha, Kashiwa,

Chiba 277-8568, Japan; imasu@aori.u-tokyo.ac.jp (R.I.);

yarai@aori.u-tokyo.ac.jp (Y.A.); satoshi.ito.1993@gmail.com (S.I.)

2 Hokkaido Research Center, Forestry and Forest Products Research Institute, 7 Hitsujigaoka, Toyohira,

Sapporo, Hokkaido 062-8516, Japan; pop128@ffpri.affrc.go.jp

3 National Institute of Advanced Industrial Science and Technology, 16-1 Onogawa, Tsukuba,

Ibaraki 305-8569, Japan; kondo-hrk@aist.go.jp

4 Japan Weather Association, 3-1-1 Higashi Ikebukuro, Toshima-ku, Tokyo 170-6055, Japan; kondo.hiroaki@jwa.or.jp

5 Earth Systems Research Center, Institute for the Study of Earth, Oceans, and Space, University of New Hampshire, Durham, NH 03824, USA; j.xiao@unh.edu

* Correspondence: qwang@aori.u-tokyo.ac.jp; Tel.:+81-4-7136-4410

This word file includes:

Supplementary text

Figures. S1 to S3

Tables S1 to S4

References cited in the Supplementary Materials are provided in the reference list of the Article.

Table S1. List of variables and their acronyms used in the sub-daily *GPP*, R_e, and *NEE* model

Symbol	Parameter name	Unit
$ALbio^x$	Biomass allocated to the part x (x=dead-wood, foliage, live-wood or root)	gC/(m²·h)
$APPFD_t$	Absorbed photosynthetic active photons flux density by the vegetation canopy at local time *t*	μmol/(m²·s)
$APPFD_{t\_y}{}^z$	Absorbed z (z=direct, scattered or diffuse) photosynthetic active photons flux density by y (y=sunlit or shaded) leaves at local time *t*	μmol/(m²·s)
bio^x	Total biomass in x (x=dead-wood, foliage, live-wood or root)	gC/m²
B_k	Empirical exponent depending on soil composition in k^{th} soil layer	-
$B_k{}^{mineral}$	Empirical exponent of mineral soil in k^{th} soil layer	-
D_0	Empirically determined coefficient to calculate g_{stCO2} (= 1000.0)	Pa
f_H	Fraction of foliage biomass consumed by herbivores	-
$f_k{}^w$	Fraction of w (w=clay, sand, silt or organic carbon) in k^{th} soil layer	-
$f_{live\text{-}wood/foliage}$	Live-wood to foliage biomass ratio	-
$f_{metabolic}$	Fraction of metabolic carbon in litter fall	-
$f_{NPPAroot}$	Fraction of *NPP* allocated to the root part	-
f_{PAV}	Fraction of $APPFD_t$ absorbed by photosynthetic active vegetation part	-
f_{Rg}	Fraction of growth respiration	-
$f_{root/foliage}$	Root to foliage biomass ratio	-
f_{sector}	A ratio of total CO_2 emission by sector in 2000 to that in 2018	-
f_{S2P}	Fraction of soil slow carbon flowing to soil passive carbon pool	-
f_{S2SM}	Fraction of soil slow carbon flowing to soil microbe carbon pool	-
f_{SM2L}	Fraction of leached soil microbe carbon	-
f_{SM2P}	Fraction of soil microbe carbon flowing to soil passive carbon pool	-
f_{SM2S}	Fraction of soil microbe carbon flowing to soil slow carbon pool	-
F_{soil1}	Limitation scalar of soil water availability on photosynthesis	-
F_{soil2}	Limitation scalar of soil hydraulic condition on transpiration,	-
F_t	Fraction of carbon loss due to microbial respiration	-
$f_t{}^y$	Fraction of y (y=sunlit or shaded) leaves at local time *t*	-
$G(\theta_t{}^{SZA})$	Projection coefficient of the leaf area	-
g_0	Stomatal conductance of CO_2 when P_n approaches 0 (= 0.01)	m/s
g_{blCO2}	Leaf boundary layer conductance of CO_2	m/s
$GridCellE_{sector}{}^{EAGrid2000Japan}$	EAGrid2000Japan CO_2 emission by sector in each grid cell	kg CO_2/s
$GridCellE_{sector}{}^{2018}$	Adjusted CO_2 emission by sector in each grid cell in 2018	kg CO_2/s
GPP	Gross Primary Production	μmol/(m²·s) or gC/(m²·h)
GPP_{BEAMS}	GPP calculated by BEAMS module	μmol/(m²·s) or gC/(m²·h)
GPP_{TLM}	GPP calculated by TLM module	μmol/(m²·s) or gC/(m²·h)
GPP_{tower}	GPP estimated from flux tower monitoring data	μmol/(m²·s) or gC/(m²·h)
g_{stCO2}	Stomatal conductance of CO_2	m/s
HCDC	High cloud cover	%
h_t	Hour angle at local time *t*	°
i	Day number of a year ([1,365] or [1,366])	-
I_{leaf}	Photosynthetic active photon absorbed by photosystem II (PSII)	μmol/(m²·s)
J	Electron transport rate to PSII	μmol/(m²·s)
J_{max}	Maximal electron transport rate to PSII	μmol/(m²·s)

Symbol	Parameter name	Unit
k	0–7 cm, 7–28 cm, 28–100 cm, and 100–289 cm	-
K_b	Extinction coefficient of $PPFD_t^{direct}$	-
K_b'	Extinction coefficient of $PPFD_t^{direct}$ accounted for leaves scattering	
K_C	Michaelis-Menten constant of Rubisco for CO_2	Pa
K_d	Extinction coefficient of $PPFD_t^{diffuse}$	-
K_d'	Extinction coefficient of $PPFD_t^{diffuset}$ accounted for leaves scattering	
K_{hc}	Hydraulic conductivity between k^{th} and $(k+1)^{th}$ soil layers	mm/s
K_{hc}^s	Saturated hydraulic conductivity between k^{th} and $(k+1)^{th}$ soil layers	
$K_{hc}^{s\_mineral}$	Saturated hydraulic conductivity of mineral soil between k^{th} and $(k+1)^{th}$ soil layers	
K_n	Extinction coefficient of leaf nitrogen content	-
K_O	Michaelis-Menten constant of Rubisco for O_2	Pa
$K_t^{diffuse}$	Clearness index (diffuse to global shortwave solar radiation ratio) at local time t	-
$L:N$	Lignin to nitrogen ratio	
LAI_t	Leaf Area Index at local time t	m^2/m^2
LAI_t^y	Total LAI of y (y=sunlit or shaded) leaves at local time t	
L_C	Effect of lignin content of structural material on structural decomposition	-
$LCDC$	Low cloud cover	%
LF^x	Litter fall from the part x (x=dead-wood, foliage, live-wood or root)	$gC/(m^2 \cdot h)$
LUE_{max}	Maximal photosynthetic light use efficiency	-
m	Empirically determined coefficient to calculate g_{stCO2} (= 4.9)	-
$MCDC$	Middle cloud cover	%
NEE	Net Ecosystem Exchange	$\mu mol/(m^2 \cdot s)$ or $gC/(m^2 \cdot h)$
N_{leaf}	Leaf nitrogen content per leaf area at specific canopy depth	g/m^2
NPP	Net Primary Production	$\mu mol/(m^2 \cdot s)$ or $gC/(m^2 \cdot h)$
N_{top}	Leaf nitrogen content per leaf area at vegetation canopy top	g/m^2
P	Photosynthetic assimilation rate	$\mu mol/(m^2 \cdot s)$
$P_{ambient}$	Surface atmospheric pressure	Pa
P_C	Rubisco limited photosynthetic assimilation rate	$\mu mol/(m^2 \cdot s)$
P_{iCO2}	Intercellular CO_2 partial pressure	Pa
P_J	Electron transport limited photosynthetic assimilation rate	$\mu mol/(m^2 \cdot s)$
P_{lsCO2}	CO_2 partial pressure at leaf surface	Pa
P_M	Photosynthetic product export and utilization limited photosynthetic assimilation rate	$\mu mol/(m^2 \cdot s)$
P_n	Net photosynthetic assimilation rate	$\mu mol/(m^2 \cdot s)$
$P_n^{big\text{-}leaf}$	Average net photosynthetic assimilation rate in big-leaf	
P_n^y	Average net photosynthetic assimilation rate in y (y=sunlit or shaded) leaves	
$PPFD_t^{direct/diffuse}$	Surface direct or diffuse photosynthetic active photons flux density at local time t	$\mu mol/(m^2 \cdot s)$
P_t^{actual}	Actual photosynthetic assimilation rate at given conditions at local time t	$\mu mol/(m^2 \cdot s)$

Symbol	Parameter name	Unit
$P_t^{optimal}$	Optimal photosynthetic assimilation rate at optimal conditions (i.e. 100% surface relative humidity and no soil water stress) at local time t	
R	Ideal gas constant	$(m^3 \cdot Pa)/(K \cdot mol)$
$R_{autotrophic}$	Autotrophic respiration rate	$gC/(m^2 \cdot h)$
R_d	Dark respiration rate at given leaf temperature	$\mu mol/(m^2 \cdot s)$
R_e	Ecosystem Respiration	$\mu mol/(m^2 \cdot s)$ or $gC/(m^2 \cdot h)$
R_{growth}	Growth respiration rate of plant	$gC/(m^2 \cdot h)$
$RH_{ambient}$	Surface relative humidity	%
$R_{heterotrophic}$	Heterotrophic respiration rate	$gC/(m^2 \cdot h)$
R_hSOC_l	Heterotrophic respiration rate of the soil organic carbon pool l (l=surface metabolic litter, surface structural litter, surface microbe, root metabolic litter, root structural litter, soil microbe, soil passive, soil slow)	
$R_{m\_base}^x$	Base maintenance respiration rate of the biomass x (x=foliage, live-wood or root)	/h
$R_{maintenance}$	Maintenance respiration rate of plant	$gC/(m^2 \cdot h)$
R_m^x	Total maintenance respiration rate of the biomass (x=foliage, live-wood or root)	
SLA	Specific leaf area	$m^2/g\ C$
SOC_l	Total biomass of the soil organic carbon pool l (l=surface metabolic litter, surface structural litter, surface microbe, root metabolic litter, root structural litter, soil microbe, soil passive, soil slow)	gC/m^2
$SR_t^{direct/diffuse}$	Surface direct or diffuse shortwave solar radiation at local time t	W/m^2
$Stress_t$	Photosynthetic stress caused by light, surface temperatures, soil moisture conditions, etc. at local time t	-
t	Local time (0,1, 2, ...,23)	-
$T_{ambient}$	Surface air temperature	K
T_k^{soil}	Temperature in k^{th} soil layer	
T_m	Effect of soil texture on SOC turnover	-
$TotalE_{sector}^{2000}$	Annual anthropogenic CO_2 emissions by sector (e.g., construction, industry, agricultural waste burning, vehicle, ship, aircraft) in Japan in 2000	ton
$TotalE_{sector}^{2018}$	Annual anthropogenic CO_2 emissions by sector (e.g., construction, industry, agricultural waste burning, vehicle, ship, aircraft) in Japan in 2018	ton
V_{cmax25}	Maximal carboxylation rate at 25°C	$\mu mol/(m^2 \cdot s)$
V_{cmax25}^{leaf}	Maximal carboxylation rate at specific canopy depth at 25°C	
V_{cmax25}^{y}	Average maximal carboxylation rate of y (y=sunlit or shaded) leaves at 25°C	
V_{cmax25}^{top}	Maximal carboxylation rate at the top of vegetation canopy at 25°C	
VP	Surface vapor pressure	hPa
VPD	Vapor pressure deficit	Pa
$\alpha_{black\text{-}sky/white\text{-}sky}$	Shortwave black-sky or white-sky albedo	-
δ	Solar declination angle on the i^{th} day of a year	°
θ_k	Water content in k^{th} soil layer	m^3/m^3

Symbol	Parameter name	Unit
θ_k^s	Saturated water content in k^{th} soil layer	
$\theta_k^{s\_mineral}$	Porosity of mineral soil in k^{th} soil layer	m^3/m^3
θ_{leaf}	Leaf response curvature to electron supply	-
θ_t^{SZA}	Cosine of solar zenith angle at local time t	-
ρ_{cb}	Vegetation canopy reflection coefficient of $PPFD_t^{direct}$	
ρ_{cd}	Vegetation canopy reflection coefficient of $PPFD_t^{diffuse}$	-
ρ_h	Vegetation canopy reflection coefficient with horizontal leaves	
σ	Vegetation canopy reflection coefficient of $PPFD$	
T	CO_2 compensation point with dark respiration	Pa
τ	Vegetation canopy transmissivity of $PPFD$	-
T^*	CO_2 compensation point without dark respiration	Pa
ϕ	Latitude of the vegetated area	°
χ_{LAD}	Empirical parameter representing leaf angle distribution	-
χ_n	Empirical coefficient of V_{cmax25} variation attributable to N_{leaf}	m^2/g
Ψ_{fc}	Soil matric water potential at field capacity (= –3.37)	
Ψ_k	Soil matric water potential in k^{th} soil layer	
Ψ_k^s	Saturated soil matric water potential in k^{th} soil layer	m
$\Psi_k^{s\_mineral}$	Saturated matric water potential of mineral soil in k^{th} soil layer	
Ψ_{wp}	Soil matric water potential at wilting point (= –152.96)	
Ω	Foliage clumping index	-

Table S2. Evaluation metrics for model calibration and validation of hourly Gross Primary Production (*GPP*), Ecosystem Respiration (R_e), and Net Ecosystem Exchange (*NEE*)

	Plant Functional Type	Group	Site	Sample size (*n*)	Standard deviation of flux tower estimates	Standard deviation of modeled results	Root mean square error	Correlation coefficient (R^2)
Hourly *GPP-BEAMS*	DBF	Calibration	SAP	12522	7.84	7.85	3.33	0.84
		Validation	API	4010	8.91	8.03	6.08	0.63
	EBF	Calibration	DIN	3857	5.41	6.00	4.59	0.53
		Validation	PSO	14650	7.37	8.59	4.56	0.72
	ENF	Calibration	FJY	8103	9.26	9.10	4.90	0.79
		Validation	QIA	7403	7.07	6.67	3.86	0.75
	GRS	Calibration	CNG	9493	5.16	4.82	3.05	0.66
		Validation	DU2	1074	3.78	4.65	4.03	0.49
Hourly GPP_{TLM}	DBF	Calibration	SAP	12522	7.84	7.66	3.26	0.83
		Validation	API	4010	8.91	7.86	5.55	0.67
	EBF	Calibration	DIN	3857	5.41	5.27	3.67	0.61
		Validation	PSO	14650	7.37	6.62	4.37	0.75
	ENF	Calibration	FJY	8336	9.21	8.79	4.41	0.79
		Validation	QIA	7403	7.07	6.30	3.75	0.74
	GRS	Calibration	CNG	9498	5.16	4.93	2.99	0.68
		Validation	DU2	1078	3.78	4.40	3.78	0.50
Hourly R_e	DBF	Calibration	SAP	78888	2.06	1.99	1.67	0.71
		Validation	API	78888	2.17	2.03	1.31	0.74
		Validation	YMS	78888	1.52	1.70	1.08	0.68
	EBF	Calibration	DIN	6238	1.76	1.64	2.04	0.25
		Validation	PSO	22344	1.71	1.20	2.61	<0.01
		Validation	YMS	78888	1.52	1.87	0.94	0.76
	ENF	Calibration	FJY	78888	2.97	2.31	1.64	0.80
		Validation	QIA	9261	2.12	1.94	1.57	0.52
	GRS	Calibration	CNG	14655	1.96	1.81	0.83	0.82
		Validation	DU2	10924	0.98	1.22	0.78	0.66
Hourly *NEE*	DBF	Calibration	SAP	78888	5.53	4.79	2.03	0.95
		Validation	API	78888	6.05	5.45	1.42	0.96
		Validation	YMS	78888	4.52	3.62	3.21	0.51
	EBF	Calibration	DIN	6238	6.76	6.45	3.28	0.80
		Validation	PSO	22344	10.21	8.88	5.43	0.74
		Validation	YMS	78888	4.52	3.99	3.37	0.50
	ENF	Calibration	FJY	78888	6.39	6.28	1.79	0.94
		Validation	QIA	9261	7.64	6.68	3.49	0.79
	GRS	Calibration	CNG	14655	3.49	3.06	1.65	0.78
		Validation	DU2	10924	1.55	1.29	1.34	0.41

[1] The unit of standard deviation and root mean square error is $\mu molCO_2/(m^2 \cdot s)$.

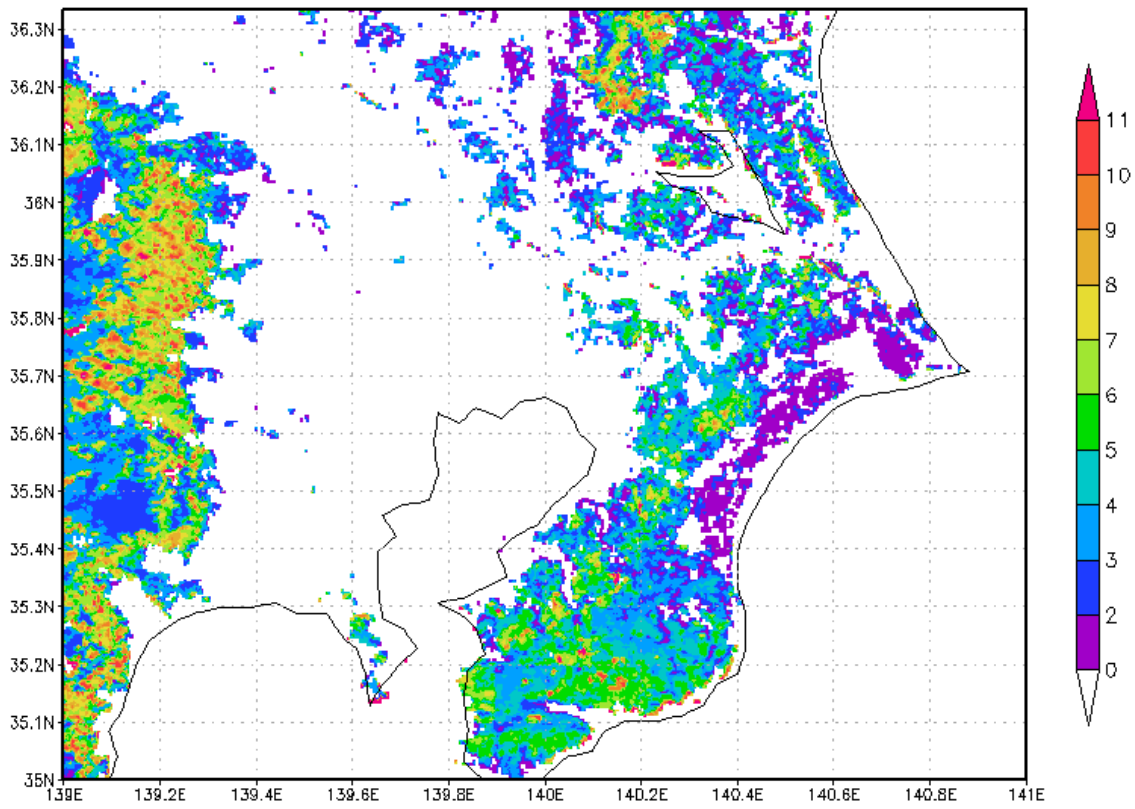

Figure S1. Accumulated carbon (sum of $SOC_{root}^{structural}$, $SOC_{root}^{metabolic}$, $SOC_{soil}^{microbe}$, SOC_{soil}^{slow}, and $SOC_{soil}^{passive}$) (kgC m^{-2}) in the 0-28 cm soil layer of the study area after model spin-up.

Calculation of hourly $SR_t^{diffuse}$

The diffuse to global shortwave solar radiation ratio (clearness index) reaching the ground at local time t is defined according to Gu et al. [51] and Jacovides et al. [54] as

$$K_t^{diffuse} = SR_t^{diffuse} / (SR_t^{direct} + SR_t^{diffuse}) \quad \text{(S1)}$$

Here, $SR_t^{diffuse}$ represents the diffuse shortwave solar radiation (W/m²) reaching the ground; SR_t^{direct} is the direct/beam shortwave solar radiation W/m² reaching the ground. To estimate $K_t^{diffuse}$, an ANN was created with eight input variables: Low Cloud Cover *LCDC* (%), Middle Cloud Cover *MCDC* (%), High Cloud Cover *HCDC* (%), surface atmospheric pressure $P_{ambient}$ (1 atm = 101325 Pa, as a proxy of elevation), shortwave black-sky albedo $\alpha_{black\text{-}sky}$, shortwave white-sky albedo $\alpha_{white\text{-}sky}$, surface vapor pressure *VP* (hPa), and the cosine of the solar zenith angle θ_t^{SZA} (90° – solar elevation angle) at local time t. Figure S2 presents a summary of the structure, layers, and nodes of ANN.

$$VP = (RH_{\text{ambient}} / 100) \times 6.1078 \times 10.0^{[7.5 \times (T_{ambient} - 273.15)] / (T_{ambient} - 273.15 + 237.3)} \quad \text{(S2)}$$

$$\cos \theta_t^{SZA} = \sin \delta \times \sin \phi + \cos \delta \times \cos \phi \times \cos h_t \quad \text{(S3)}$$

$$\delta = 23.44° \times \cos [2\pi \times (i+193) / 365] \quad \text{(S4)}$$

$$h_t = 15° \times (t - 12) \quad \text{(S5)}$$

Here, $T_{ambient}$ represents the surface air temperature (K), $RH_{ambient}$ denotes the surface relative humidity (%), ϕ stands for latitude (°), δ signifies the solar declination angle on the i^{th} day of a year, and h_t represents the hour angle.

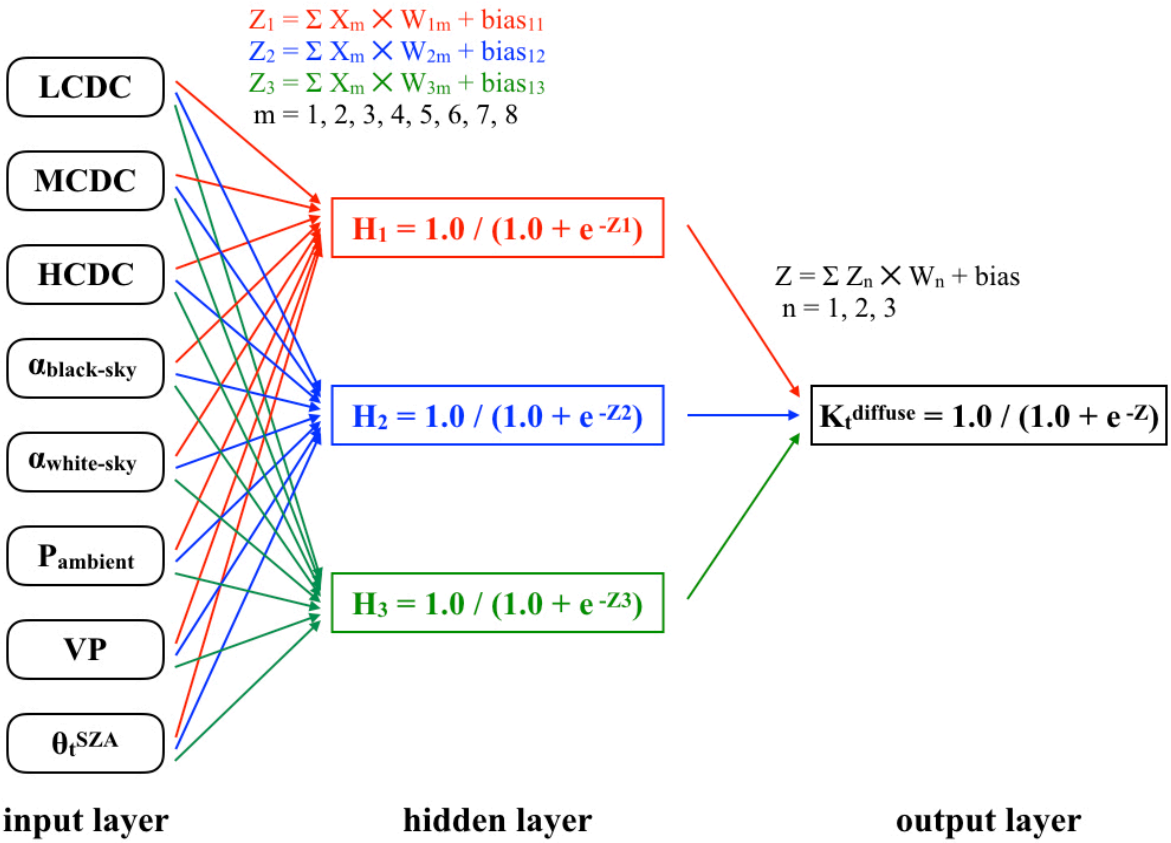

Figure S2. Structure, layers, and nodes of Artificial Neural Network (ANN) to estimate $K_t^{diffuse}$.

To train the ANN, hourly averaged $SR_t^{diffuse}$ and SR_t^{global} ($SR_t^{diffuse}$ + SR_t^{direct}) of 2014– 2019 were extracted from three World Radiation Data Centre (WRDC, [164]) sites (Fukuoka, 130.38°E 33.58°N; Tateno, 140.13°E 36.05°N; and Sapporo, 141.33°E 43.07°N) to calculate the observed $K_t^{diffuse}$. The Adam algorithm of the Python keras library was applied to reduce the error between observed $K_t^{diffuse}$ and the predicted $K_t^{diffuse}$. To avoid unrepresentative validation, validation split of hourly samples was set to 0.5. To avoid overfitting, early stopping in the Python keras library was used to monitor the model performance and halt training when the decrease of root mean square error (RMSE) stabilized. Table S3 presents the calibrated parameters in the ANN.

Table S3. Parameters to activate the ANN and predict $K_t^{diffuse}$

		H_1	H_2	H_3
Weights to predict $H_{1,2,3}$	X_1 (*LCDC*)	-1.3717216	3.9363568	-2.9427488
	X_2 (*MCDC*)	-2.4580557	3.1441848	-2.2686243
	X_3 (*HCDC*)	-1.0388604	1.8021374	-1.7345482
	X_4 ($\alpha_{black\text{-}sky}$)	-1.0298406	1.0571014	-1.0376163
	X_5 ($\alpha_{white\text{-}sky}$)	0.2406344	0.41680366	0.35457167
	X_6 ($P_{ambient}$)	-0.24406493	-0.26760823	0.19336297
	X_7 (*VP*)	0.03414719	-0.01849018	0.06454528
	X_8 (θ_t^{SZA})	1.2372994	-1.5896108	0.16927624
Biases to predict $H_{1,2,3}$		0.14815871	-0.39750978	0.05327982
Weights to predict Z		-1.1487454	2.6597986	-1.2089859
Bias to predict Z			0.46301052	

To evaluate the ANN performance, the modeled $SR_t^{diffuse}$ (calculated $K_t^{diffuse}$ × observed SR_t^{global}) was compared with the observed $SR_t^{diffuse}$ at the WRDC sites, which is summarized by the Taylor diagram in Figure S3. The ANN modeled hourly $SR_t^{diffuse}$ generally showed good agreement with observations. The centered pattern of modeled and measured $SR_t^{diffuse}$ variations was similar (> 0.7). The coefficient of determination (R^2) was 0.63 at the Fukuoka site (WRDC-F, sample size =25689), 0.58 at the Tateno site (WRDC-T, sample size =26254), and 0.62 at the Sapporo site (WRDC-S, sample size =25628). The RMSE between the hourly observed $SR_t^{diffuse}$ and estimation at the Sapporo site was 102.67 W/m², which was higher than that at the Tateno site (89.13 W/m²) and the Fukuoka site (88.00 W/m²). The standard deviations of hourly modeled $SR_t^{diffuse}$ was slightly larger than the observed ones, which were, respectively, 138.04 and 120.63 W/m² (WRDC-T), 142.02 and 118.59 W/m² (WRDC-F), and 149.58 and 113.20 W/m² (WRDC-S).

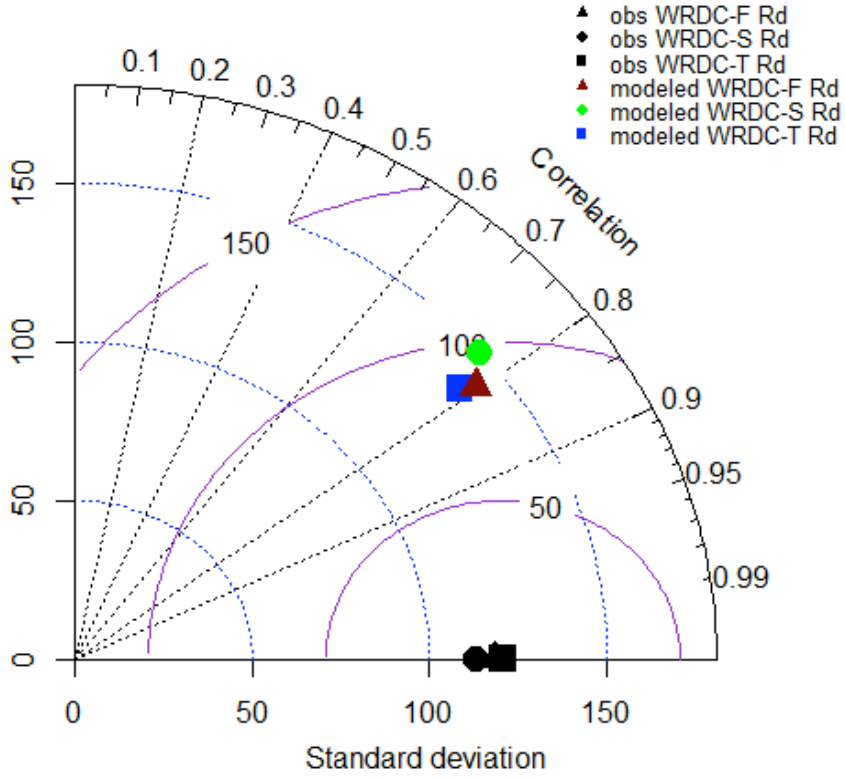

Figure S3. Taylor diagram of hourly observed and modeled $SR_t^{diffuse}$ (W m^{-2}) at the World Radiation Data Centre Fukuoka, Sapporo, and Tateno sites.

Calculation of hourly APPDF$_t$

With solved $K_t^{diffuse}$, the $PPFD_t^{diffuse}$ and $PPFD_t^{direct}$ were calculated based on equation A10 proposed by Ito and Oikawa [65]. Then $APPFD_t$ was estimated using equations 20b ($APPFD_{t\_sunlit}^{direct}$), 20c ($APPFD_{t\_sunlit}^{diffuse}$), 20d ($APPFD_{t\_sunlit}^{scattered}$), A26b ($APPFD_{t\_shaded}^{diffuse}$), A26c ($APPFD_{t\_shaded}^{scattered}$), A4 ($K_b'$, K_d'), A19 (ρ_{cb}), A20 (ρ_h), A21 (ρ_{cd}) deduced by de Pury and Farquhar [55]. In the sunlit/shaded leaves model with clumping index Ω representing the randomness of leaf distribution, we assumed a planophile or plagiophile leaf angle (χ_{LAD}=1.0) in broadleaf forests according to Pisek et al. [165] and a spherical leaf angle (χ_{LAD}=0.0) in needleleaf forests and grasslands according to Stenberg [166] and Luo et al. [58]. The extinction coefficient of $PPFD_t^{direct}$, K_b can be expressed as follows:

$$K_b = G(\theta_t^{SZA}) \times \Omega \,/\, cos\ \theta_t^{SZA} \quad \text{(S6)}$$

where $G(\theta_t^{SZA})$ is the projection coefficient of the leaf area, as described by equation A4 reported by Sellers et al. [167].

Quality control screening and interpolation of the Leaf Area Index

The *LAI* is a key variable for estimating the total photosynthetic active leaf area (*GPP* module) and foliage biomass (R_e module). To remove cloud-contaminated data, only MODIS *LAI* (MCD15A3H v006 [107], 4-day 500 m) values for

which the quality control layer FparLai_QC equaled to 0/2/32/34 were retained. In DBF and GRS, the *LAI* trend over time was constrained by phenological metrics such as the date of Greenup, Peak, and Dormancy provided by the MODIS Land Cover Dynamics dataset (MCD12Q2 v006 [119], annual 500 m). To be more specific, abnormal decline (< -0.5 (m^2/m^2)/4-day) during the leaf green-up to peak period or abnormal increase of *LAI* (> 0.5 (m^2/m^2)/4-day) during the peak to leaf dormancy period was neglected. Gaps of *LAI* in forest, grassland, and urban vegetated land were then filled via temporal linear averaging interpolation [168].

Simplified Farquhar – von Caemmerer – Berry model

In C3 plants under the given meteorological conditions, the net photosynthetic assimilation rate P_n (μmol/(m^2·s)) of sunlit (P_n^{sunlit}), shaded (P_n^{shaded}) or big-leaf ($P_n^{big\text{-}leaf}$) was quantified using a simplified Farquhar – von Caemmerer – Berry model using equations 3 (P), 4 (P_C), 5 (P_J), 6 (P_M), and 15 (P_n) presented by Sasai et al. [69], with intermediate variables described by equations A1 (N_{leaf}), A2 (V_{cmax25}^{leaf}), A3 (f_t^{sunlit} and consequently LAI_t^{sunlit}), A4 (f_t^{shaded} and consequently LAI_t^{shaded}), A5 (V_{cmax25}^{sunlit}), and A6 (V_{cmax25}^{shaded}) in Luo et al. [58], equations 7 (K_C), 8 (K_O), 9 (V_{cmax}), 10 (F_{soil1}), 11 (Ψ), 12&13 (T^*), and 19 (F_{soil2}, Ψ_{wp} set to -152.96 m / 1500 kPa and Ψ_{fc} to -3.37 m / 33 kPa according to Saxton and Rawls [169]) from Sasai et al. [69], equation 16 (R_d) in Sellers et al. [75], equations 7.81 (θ_k^s), 7.82 ($\theta_k^{s\_mineral}$), 7.83 (B_k), 7.84 (B_k^{mineral}), 7.86 (Ψ_k^s), and 7.87 ($\Psi_k^{s\_mineral}$) from Oleson et al. [170], equation 5 (J) from de Pury and Farquhar [55], whereas the maximal electron transport rate $J_{\max}$ was estimated based on Wullschleger [76] as

$$J_{max} = 1.64 \times V_{cmax} + 29.1 \tag{S7}$$

To estimate the flux density of photosynthetic active photon absorbed effectively by Photosystem II in leaf chloroplasts (I_{leaf}), which is a key variable to estimate J, a scaling factor f_{PAV} was introduced to calculate the amount of *APPFD* absorbed by the photosynthetic active leaf part in each PFT.

$$I_{leaf} = 0.5 \times f_{PAV} \times (APPFD / LAI) \tag{S8}$$

Stomatal and leaf surface conductance of CO_2

The intercellular CO_2 supply is controlled by stomata in C3 plants. According to Fick's law, the net exchange of CO_2 between a leaf surface (where CO_2 partial pressure is denoted as P_{lsCO2} (Pa)) and its intercellular environment (where CO_2 partial pressure is denoted as P_{iCO2} (Pa)) is driven by the gradient of CO_2 concentration and stomatal conductance of CO_2 (g_{stCO2}). This relation is based on the ideal gas law, equation 16.9 and 16.10 in Bonan [77] and can be expressed as follows:

$$P_{iCO2} = P_{lsCO2} - (R \times T_{ambient} \times P_n / g_{stCO2}) \tag{S9}$$

$$P_{lsCO2} = P_{ambientCO2} - (P_n / g_{blCO2}) \tag{S10}$$

Therein, R is the ideal gas constant. The temperatures at the leaf surface and in its intercellular environment were assumed with ambient value for this study. The value of g_{blCO2} is the leaf boundary layer conductance of CO_2, assumed as 1/1.4 of leaf boundary layer conductance of water vapor, which can be solved by equation 15.3 in Bonan [77]. According to Leuning [79], g_{stCO2} is

$$g_{stCO2} = g_0 + (m \times F_{soil2} \times R \times T_{ambient} \times P_n) / [(P_{lsCO2} - T) \times (1.0 + VPD / D_0)] \tag{S11}$$

where g_0 (0.01 m/s) is the CO_2 stomatal conductance when P_n approaches 0. Also, m (4.9) and D_0 (1000.0) are empirically determined coefficients for *Quercus suber* in Leuning [79]. T is the CO_2 compensation point with dark respiration, solved using equation 11 in Leuning [78]. The vapor pressure deficit (*VPD*) is solved by equation 3.32 in Bonan [77]. The equation of saturated vapor pressure was referred from page 348 of Jones [80].

Iteration to solve photosynthetic assimilation rate

To solve the photosynthetic assimilation rates and P_{iCO2}, the following iterative method was applied.

- Set initial P_{iCO2} to 0.7 of the partial pressure of ambient atmospheric CO_2.
- Calculate P_C, P_J, and P_M accordingly to solve P_n.
- Calculate P_{lsCO2} and g_{stCO2}.
- Update P_{iCO2} using solved variables in steps 2 and 3.
- If the change of P_{iCO2} is negligible (<0.001 Pa in this study), P_{iCO2} and P_n are considered solved; otherwise, apply the updated P_{iCO2} to repeat step 2–5. To avoid infinite loops, iterations were limited to 100.

Allocation of Net Primary Production carbon

For this study, vegetation biomass pools were simplified to foliage biomass, wood (live-wood and dead-wood) biomass, and root biomass pools in DBF, EBF, and ENF, and foliage biomass and root biomass pools in GRS. With a given LAI_t at local time t, each biomass pool was estimated based on equation 1.4 ($bio_t^{foliage}$), 1.5 (bio_t^{root}), and 1.9 ($bio_t^{live\text{-}wood}$) from Heinsch et al. [82], except in DBF, where some live roots might remain active and respire even if LAI_t appears to be 0 in early spring or late autumn. When hourly *NPP* exceeded the cost of total growth in foliage and live-wood biomass in DBF, the rest would be allocated to bio_t^{root} and $bio_t^{dead\text{-}wood}$.

$$bio_{t+1}^{root} = bio_t^{root} + (NPP - ALbio_{foliage} - ALbio_{live\text{-}wood}) \times f_{NPPAroot} - R_m^{root} - LF_{root} \quad \text{(S12)}$$

where $ALbio_{foliage}$ is the biomass amount allocated to the foliage part (if $LAI_t < LAI_{t+1}$, $ALbio_{foliage}$ equals [($bio_{t+1}^{foliage}$ based on LAI_{t+1} – $bio_t^{foliage}$ based on LAI_t) × (1.0 + f_H) + $R_m^{foliage}$]; if $LAI_{t+1} < LAI_t$ but ($bio_t^{foliage}$ based on LAI_t – $bio_{t+1}^{foliage}$ based on LAI_{t+1}) < [($bio_t^{foliage}$ based on LAI_t – $bio_{t+1}^{foliage}$ based on LAI_{t+1}) × f_H + $R_m^{foliage}$], $ALbio_{foliage}$ equals [($bio_t^{foliage}$ based on LAI_t – $bio_{t+1}^{foliage}$ based on LAI_{t+1}) × (f_H –1.0) + $R_m^{foliage}$]). Here, f_H is the fraction of foliage biomass consumed by herbivores (0.134 in DBF and EBF, 0.068 in ENF, and 0.109 in GRS, Randerson et al. [155]); $ALbio_{live\text{-}wood}$ represents the biomass allocated to the live-wood part (if $LAI_t < LAI_{t+1}$, $ALbio_{live\text{-}wood}$ equals [($bio_{t+1}^{live\text{-}wood}$ based on LAI_{t+1} – $bio_t^{live\text{-}wood}$ based on LAI_t) + $R_m^{live\text{-}wood}$]; if $LAI_{t+1} < LAI_t$ but ($bio_t^{live\text{-}wood}$ based on LAI_t – $bio_{t+1}^{live\text{-}wood}$ based on LAI_{t+1}) < $R_m^{live\text{-}wood}$, $ALbio_{live\text{-}wood}$ equals to [$R_m^{live\text{-}wood}$ – ($bio_t^{live\text{-}wood}$ based on LAI_t – $bio_{t+1}^{live\text{-}wood}$ based on LAI_{t+1})]). Also, $f_{NPPAroot}$ is the fraction of *NPP* allocated to roots, as calculated using equations 2 and 5 from Friedlingstein et al. [84]. Because of the lack of measurements, the resource availability scalar of nitrogen was assumed to be unlimited (=1). LF_{root} is the hourly root litter fall, assumed as 1.30×10^{-6} of bio_t^{root}in DBF according to hourly values converted from Ito and Oikawa [171].

In cases where the hourly *NPP* exceeded the total cost of foliage, live-wood, and root biomass growth ($ALbio_{root}$ is the biomass allocated to root part (if $LAI_t < LAI_{t+1}$, $ALbio_{root}$ equals [(bio_{t+1}^{root} based on LAI_{t+1} – bio_t^{root} based on LAI_t) + R_m^{root}]; if $LAI_{t+1} < LAI_t$ but (bio_t^{root}based on LAI_t – bio_{t+1}^{root} based on LAI_{t+1}) < R_m^{root}, $ALbio_{root}$ equals to [R_m^{root} – (bio_t^{root} based on LAI_t – bio_{t+1}^{root} based on LAI_{t+1})]), the rest is assigned to the dead-wood biomass pool.

$$bio_{t+1}^{dead\text{-}wood} = bio_t^{dead\text{-}wood} + (NPP - ALbio_{foliage} - ALbio_{live\text{-}wood} - ALbio_{root}) - LF_{dead\text{-}wood} \quad \text{(S13)}$$

where $LF_{dead\text{-}wood}$ is the hourly deadwood litter fall (2.15×10^{-6} of $bio_t^{dead\text{-}wood}$ in DBF and EBF, 8.3×10^{-7} of $bio_t^{dead\text{-}wood}$ in ENF according to hourly values converted from those parameter settings by Ito and Oikawa [171]).

Maintenance respiration rate of vegetation

Maintenance respiration rates under ambient temperature conditions were calculated based on equations 1.6 ($R_m^{foliage}$), 1.7 (R_m^{root}), and 1.10 ($R_m^{live\text{-}wood}$) from Heinsch et al. [82]. Q_{10Rm} was set to 1.4 according to Mahecha et al. [172], whereas other PFT-specific parameters are presented in Table S3.

Foliage and wood litter fall consists of soil surface litter biomass. If $LAI_{t+1} < LAI_t$ and ($bio_t^{foliage}$ based on LAI_t – $bio_{t+1}^{foliage}$ based on LAI_{t+1}) > [($bio_t^{foliage}$ based on LAI_t – $bio_{t+1}^{foliage}$ based on LAI_{t+1}) × f_H + $R_m^{foliage}$], then the following equations are used.

$$LF_{foliage} = (bio_t^{foliage} \text{ based on } LAI_t - bio_{t+1}^{foliage} \text{ based on } LAI_{t+1}) \times (1 - f_H) - R_m^{foliage} \quad \text{(S14)}$$

If $LAI_{t+1} < LAI_t$ and ($bio_t^{live\text{-}wood}$ based on LAI_t – $bio_{t+1}^{live\text{-}wood}$ based on LAI_{t+1}) > $R_m^{live\text{-}wood}$, then

$$LF_{live\text{-}wood} = (bio_t^{live\text{-}wood} \text{ based on } LAI_t - bio_{t+1}^{live\text{-}wood} \text{ based on } LAI_{t+1}) - R_m^{live\text{-}wood} \quad \text{(S15)}$$

Litter fall of roots in evergreen forests and grasslands was calculated using an equation similar to S15. A 5% [64] loss of foliage and root litter was also set to subtract quickly dissolved soluble matter, which does not contribute to CO_2 emissions because of organic carbon decomposition.

Table S4. PFT-specific parameters used to calculate hourly $R_{maintenance}$

Symbol	Parameter	Unit	Plant Functional Type			
			DBF	EBF	ENF	GRS
SLA	Specific leaf area	m^2/g C	0.0218	0.0259	0.0141	0.0375
$f_{live\text{-}wood/foliage}$	Live-wood to foliage biomass ratio	-	0.203	0.162	0.182	-
$f_{root/foliage}$	Root to foliage biomass ratio	-	-	1.1	1.2	2.6
$R_{m\_base}^{foliage}$	Base maintenance respiration rate of foliage	/hr	0.000324	0.000252	0.000252	0.000408
$R_{m\_base}^{live\text{-}wood}$	Base maintenance respiration rate of live-wood	/hr	0.000155	0.000165	0.000165	-
$R_{m\_base}^{root}$	Base maintenance respiration rate of root	/hr	0.000216	0.000216	0.000216	0.000341

Dynamics of carbon in SOC pools

Finally, the calculation of carbon flow in *SOC* pools was done following Figure 1 presented by Parton et al. [87] and Figure 2 from Bonan et al. [88]. Intermediate variables in this part were quantified using equations 5 (T_m), 6 (L_C), 7 (F_t), 8 (f_{SM2L}), 9 (f_{SM2P}), 10 (f_{SM2S}), 11 (f_{S2P}), and 12 (f_{S2SM}) from Parton et al. [87]; abiotic scalars of soil temperature and moisture conditions on SOC decomposition rates were calculated using equations 5, 6, 7, and 8 from Ise and Moorcroft [173] plus equations 18, 19, 20, and 21 presented by Cox [174]. Hydraulic conductivity mm/s between soil layers (K_{hc}) replaced the monthly saturated water flow to estimate leached carbon, following equations 7.80 (K_{hc}), 7.90 ($K_{hc}^{s\_mineral}$), and 7.91 (K_{hc}^{s}) from Oleson et al. [170]. In terms of the metabolic carbon fraction in litter falls, it was assumed to be related to *L:N*, the lignin nitrogen ratio (37.8 in broadleaf forests, 58.8 in needleleaf forests, and 25.5 in GRS according to Osono and Takeda [175]).

$$f_{metabolic} = 0.85 - 0.013 \times L{:}N \quad \text{(S16)}$$

Because of the lack of measurements in our study area, the maximal hourly decomposition rate of each *SOC* and fractions of respired CO_2 were set to hourly values converted from Bonan et al. [88].